doi:10.1016/j.jmb.2010.08.005 J. Mol. Biol. (2010) 403, 331–345

Contents lists available at www.sciencedirect.com

Journal of Molecular Biology

journal homepage: http://ees.elsevier.com.jmb

Quantitative Proteomic Analysis of Ribosome Assembly and Turnover *In Vivo*

Michael T. Sykes†, Zahra Shajani†, Edit Sperling, Andrea H. Beck and James R. Williamson*

Departments of Molecular Biology and Chemistry and the Skaggs Institute for Chemical Biology, The Scripps Research Institute, MB-33, 10550 North Torrey Pines Road, La Jolla, CA 92037, USA

Received 8 July 2010;
received in revised form
26 July 2010;
accepted 2 August 2010
Available online
13 August 2010

Edited by D. E. Draper

Keywords:
ribosome assembly;
assembly intermediates;
quantitative mass spectrometry;
proteomics;
RNA–protein interactions

Although high-resolution structures of the ribosome have been solved in a series of functional states, relatively little is known about how the ribosome assembles, particularly *in vivo*. Here, a general method is presented for studying the dynamics of ribosome assembly and ribosomal assembly intermediates. Since significant quantities of assembly intermediates are not present under normal growth conditions, the antibiotic neomycin is used to perturb wild-type *Escherichia coli*. Treatment of *E. coli* with the antibiotic neomycin results in the accumulation of a continuum of assembly intermediates for both the 30S and 50S subunits. The protein composition and the protein stoichiometry of these intermediates were determined by quantitative mass spectrometry using purified unlabeled and ^{15}N-labeled wild-type ribosomes as external standards. The intermediates throughout the continuum are heterogeneous and are largely depleted of late-binding proteins. Pulse-labeling with ^{15}N-labeled medium time-stamps the ribosomal proteins based on their time of synthesis. The assembly intermediates contain both newly synthesized proteins and proteins that originated in previously synthesized intact subunits. This observation requires either a significant amount of ribosome degradation or the exchange or reuse of ribosomal proteins. These specific methods can be applied to any system where ribosomal assembly intermediates accumulate, including strains with deletions or mutations of assembly factors. This general approach can be applied to study the dynamics of assembly and turnover of other macromolecular complexes that can be isolated from cells.

Introduction

The ribosome is a complex macromolecular machine composed of three strands of RNA and more than 50 proteins. Although high-resolution crystal structures of the ribosome in numerous conformations and complexes have been solved,[1–3] relatively little is known about how the various ribosomal components assemble into complete ribosomes. Much of the knowledge about assembly comes from experiments performed *in vitro*,

*Corresponding author. E-mail address: jrwill@scripps.edu.

† M.T.S. and Z.S. contributed equally to this work.

Abbreviations used: LC/MS, liquid chromatography-coupled mass spectrometry; EDTA, ethylenediaminetetraacetic acid; TCA, trichloroacetic acid; ACN, acetonitrile; ESI-TOF, electrospray ionization time-of-flight.

beginning with seminal work on thermodynamic protein binding hierarchies in both the 30S[4,5] and 50S[6] subunits. However, *in vitro* studies such as these do not account for either the numerous assembly factors present *in vivo*[7] or the co-transcriptional nature of assembly in the cell.[8,9]

One of the major outstanding questions about ribosome assembly is whether assembly occurs via a single pathway or via multiple parallel assembly trajectories, though recent *in vitro* work involving pulse-chase kinetic assays[10,11] and time-resolved hydroxyl radical footprinting[12] suggest the latter. Even so, the number of pathways and the composition of the intermediates populated along these pathways remain unknown.

In the current work, a general method is presented for the analysis of incomplete and complete ribosomal particles assembled *in vivo*. The only putative *in vitro* assembly intermediates that have been identified for 30S ribosome assembly are RI and RI*.[13,14] Comparison of footprinting data for 16S rRNA in RI, RI*, and 30S particles reveals specific differences in RNA conformations,[15,16] but the relevance of the RI particles for assembly *in vivo* remains unclear.[17] Unfortunately, due to the relative difficulty of reconstituting 50S subunits *in vitro*, similar studies have not been performed on the large ribosomal subunit. However, the abundance of cofactors involved in 50S assembly[7] has offered the opportunity to study intermediates induced as a result of cofactor disruption, including those resulting from the deletion of SrmB,[18] CsdA,[19] and DnaK or DnaJ,[20] and mutations to $CgtA_E$[21] and DbpA.[22] The diverse range of intermediates observed in this set of deletion strains implies a rich and complex assembly mechanism for the 50S subunit.

Ribosomal assembly intermediates are not plentiful under normal growth conditions and are therefore difficult to purify and study. Chemicals and mutations are standard ways of perturbing complex pathways, in order to dissect the underlying mechanism. The antibiotic neomycin has been proposed to be an assembly inhibitor,[23,24] and in this work, a pulse with sublethal concentrations of neomycin is used as a simple and efficient chemical inhibitor to generate ribosomal assembly intermediates whose composition can be determined using quantitative proteomic mass spectrometry. While earlier work involving neomycin identified a single 21S precursor to the 30S subunit,[25] in the present work, a continuum of assembly intermediates for both the 30S and 50S subunits is observed. Previous work using different antibiotics has established a precedent for the inhibition of 50S assembly by antibiotics.[26,27] The composition of the precursor particles for both the 30S and 50S subunits was analyzed throughout the continuum, and a heterogeneous population was observed at each point in the continuum, containing all of the ribosomal proteins in varying amounts. This continuum of intermediates begins with particles containing very low levels of each ribosomal protein, progressing to intact subunits. Furthermore, the intermediates were shown to contain proteins synthesized before the addition of neomycin to the culture, indicating that some amount of the proteins originated in previously existing intact subunits.

These observations are made possible by novel applications of quantitative proteomic mass spectrometry. In a protein inventory experiment, both unlabeled and fully ^{15}N-labeled 70S ribosomes are added as external standards to a 50% ^{15}N-labeled sample particle. The identification and quantitation of tryptic peptides are decoupled using a strategy developed to identify ribosomal peptides via unlabeled and labeled peak pairs.[11,28,29] In this way, extremely low levels of ribosomal proteins in the test sample can be accurately quantitated in assembly intermediates. In a pulse-labeling experiment, an isotope pulse time-stamps proteins based on their time of synthesis, providing information about the temporal origins of the proteins in different ribosomal particles. In both experiments, the quantitative analysis is made possible by least-squares Fourier transform convolution,[30] which enables the relative quantitation of mixtures of arbitrarily labeled peptides, including the 50% ^{15}N-labeled species.

Results

Precursors to both small and large subunits accumulate in *Escherichia coli* treated with neomycin

E. coli grown in the presence of sublethal concentrations of neomycin accumulate precursors to both the 30S small subunit and the 50S large subunit. Traces from sucrose gradient ultracentrifugation of cell lysate are shown for untreated cells and neomycin-treated cells in Fig. 1a and b, respectively. In the untreated cells, two small peaks are observed early in the gradient arising from cell debris, and two prominent peaks are observed for 30S and 50S subunits. In the treated cells, the 30S precursor is visible as a distinct peak in the gradient at the location of a 21S particle (Fig. 1b), as reported previously.[23–25] In addition, a previously unreported 50S precursor co-sediments with the 30S subunit, as revealed by agarose gel electrophoresis analysis that demonstrates the presence of 23S ribosomal RNA (rRNA) in the 30S peak (Fig. 1b). In contrast, cells grown without neomycin do not have a 21S peak in the sucrose gradient and have no detectable amounts of 23S rRNA within the 30S peak. The addition of neomycin also causes an

accumulation of 70S ribosomes (Fig. 1b) that, unlike in the control cells, do not completely dissociate into 30S and 50S subunits under the dissociating conditions used for ultracentrifugation. This phenomenon has not been previously observed to our knowledge and is not further investigated in this work.

Assembly intermediates are heterogeneous particles with low protein occupancy

The protein levels for ribosomal proteins in sucrose gradient fractions corresponding to assembly intermediates and intact ribosomal subunits were measured relative to the ^{14}N- and ^{15}N-70S ribosome external standards (see Materials and Methods). The magnitudes of the initial protein levels are implicitly dependent on the amount of standard added; thus, they are scaled based on the relative amount of rRNA in the fraction as determined by quantifying agarose gel spot intensities. Direct absorbance measurements from the fractions were not used for scaling as they include a significant and indeterminate contribution from DNA and contaminating proteins that varies from fraction to fraction. A fraction from the center of the 30S peak (Fig. 1b, fraction 10) is scaled such that the average occupancy is 1.0 for 30S proteins, and 30S proteins in all other fractions are scaled relative to this. 50S proteins are treated in a similar manner by scaling based on a single fraction from the center of the 50S peak (Fig. 1b, fraction 16). Assuming a 1:1 protein-to-rRNA correspondence in the standards, the scaled values represent the fraction of 16S or 23S rRNA molecules that have a particular protein bound. A scaled protein level of 0.5 indicates that only 50% of the rRNA molecules have that particular protein bound.

Protein levels for 30S proteins present in fractions 6 and 11, corresponding to the centers of the 21S and 30S peaks, respectively, are shown in Fig. 2a. For the 30S peak, all proteins are present with a level of approximately 1, indicating homogenous, intact particles. For the 21S peak, protein levels are much lower and vary widely from protein to protein. Primary binding proteins from the central domain (S8 and S15) are present in the highest levels (~13–14%), while tertiary binding proteins (S2, S3, S5, S12, and S21) are present at the lowest levels (~2–3%). This variation indicates a heterogeneous collection of particles that sediment at the same general location in the gradient. Interestingly, the central domain appears to be most complete, with the

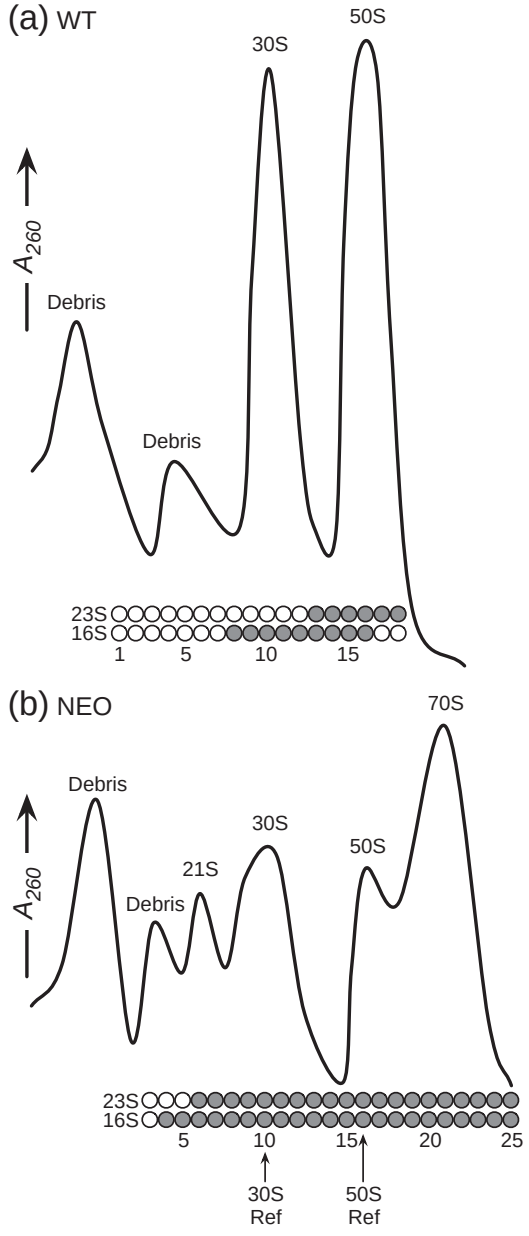

Fig. 1. Sucrose gradient ultracentrifugation profiles of cell lysate and gel electrophoresis of rRNA. (a) A dissociating sucrose gradient of log phase *E. coli*. Circles indicate fractions tested for rRNA by agarose gel electrophoresis. Shaded circles indicate the presence of either 16S or 23S rRNA. Clearly visible in the sucrose gradient trace are prominent peaks due to 30S and 50S subunits. Two small peaks are attributed to cell debris, appear in all gradients, and do not contain any rRNA. The 16S rRNA is found only in the 30S peak fractions, and the 23S rRNA is found only in the 50S peak fractions. (b) A dissociating sucrose gradient of *E. coli* treated with neomycin. Additional peaks appear in the sucrose gradient trace at 21S and 70S and the 30S peak broadens. Both 16S and 23S rRNA are found in earlier gradient fractions compared to the log phase unperturbed culture and persist throughout. Fraction 10 was used as the reference fraction for scaling the 30S subunit protein levels and fraction 16 was used as the reference fraction for scaling the 50S subunit protein levels.

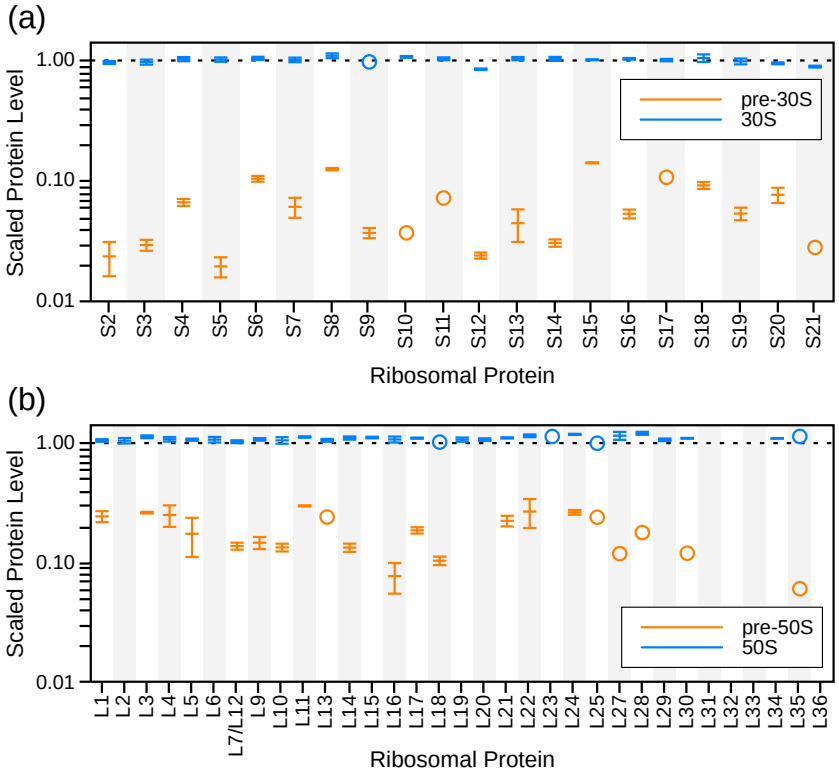

Fig. 2. Scaled protein levels for the 30S and 50S subunits and assembly intermediates. (a) Protein levels from a single fraction from the 30S subunit peak (blue; Fig. 1b, fraction 11) and protein levels from a single fraction from the 21S intermediate peak (orange; Fig. 1b, fraction 6). A log scale is used for the *y*-axis to highlight the differences among protein levels in the 21S intermediate, which are less than ~10% of the protein levels in the intact 30S subunits. Values are scaled to represent the occupancy relative to the amount of rRNA as described in Materials and Methods. Error bars represent the standard deviation of multiple measurements from different peptides or ions of the same protein. In the case where a single measurement was obtained, an open circle is used. (b) Protein levels from a single fraction of the 50S subunit peak (blue; Fig. 1b, fraction 17) and protein levels from a single fraction of the 30S peak, representing the pre-50S assembly intermediate (orange; Fig. 1b, fraction 12).

secondary binding proteins S6 and S18 present at the same level or higher (~10%) than primary binding proteins in the 5′ domain.

Protein levels for 50S proteins present in fractions 12 and 17, corresponding to the 30S and 50S peaks, respectively, are shown in Fig. 2b. All of the large subunit proteins in the 50S peak are present with a level of approximately 1, indicating a complete, homogenous 50S subunit. However, 50S proteins in the 30S peak are present at lower levels (~6–12%) that vary from protein to protein. In the fraction shown, some of the smaller large subunit proteins were not identified, but only L36 was not identified in any of the fractions tested. As with the small subunit, the varied protein level indicates a heterogeneous collection of assembly intermediates with overall low levels of proteins. The low protein levels in the case of both precursor particles indicate that, on the whole, each rRNA molecule has very few proteins associated with it.

There is a continuum of incomplete particles in neomycin-treated cells

Protein levels for ribosomal proteins in fractions collected through the entire sucrose gradient were measured using liquid chromatography-coupled mass spectrometry (LC/MS). Fractions corresponding to smaller sedimentation coefficients contained low levels of ribosomal proteins, and traversing across the sucrose gradient from lower to higher sedimentation coefficients revealed a steady increase in protein levels. Interestingly, although the small subunit proteins each peaked at a level of 1 in the center of the 30S peak, the rate of increase varied for different proteins. Based on this rate of increase, it is possible to group the proteins of the small ribosomal subunit into three categories: early binders (S6, S8, S15, S17, and S18), moderate binders (S4, S7, S9, S10, S11, S13, S14, S16, S19, and S20), and late binders (S2, S3, S5, S12, and S21). Plots for representative proteins

from each of the three groups (early: S15, moderate: S7, late: S3) are shown in Fig. 3a, and plots for all 30S proteins are shown in Supplementary Figs. S1 and S2. The separation between the three groups is clearly visible in Supplementary Fig. S1, fraction 7. The Nomura assembly map[5] is colored based on these three groups and is shown in Fig. 3b. As indicated by the protein levels from a single fraction, the central domain is the most completely assembled in these intermediates.

The protein levels for the large subunit proteins peaked in fractions taken from the center of the 50S peak and displayed variations in the rate of increase similar to those seen in the small subunit. The large subunit proteins do not fall into three clear groups; hence, they are split into three groups of equal size based on their scaled protein level in fraction 13. No data were obtained for L20, L32, and L36 in fraction 13; thus, they are placed in the late binding group. Plots for representative proteins from each of these three groups (early: L4, moderate: L5, late: L35) are shown in Fig. 3c, and plots for all 50S proteins are shown in Supplementary Figs. S3 and S4. The Nierhaus assembly map[6] is colored based on these three groups and is shown in Fig. 3d. While the map lacks the simple domain structure of the Nomura assembly map for the 30S subunit, the three groups still correlate well with the defined order of assembly. Early binders are primarily primary binding proteins, while the late binders are generally tertiary binding proteins.

Interestingly, intermediates are plentiful in each of the fractions shown here, based on quantitation of gel spots from agarose gel electrophoresis (data not shown), and the variation in the amount of rRNA between fractions is relatively small. From fraction

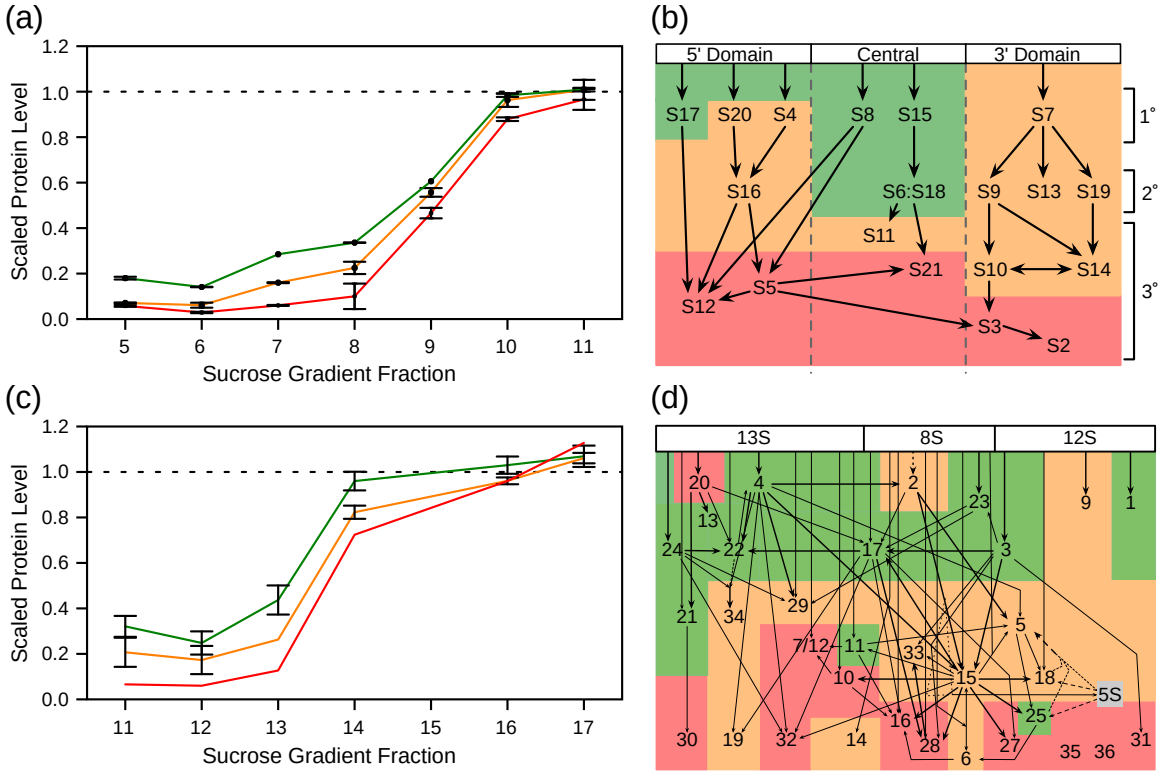

Fig. 3. Changes in protein levels across different fractions in the sucrose gradient, and protein levels correlated with assembly maps. (a) Curves for representative proteins from the 30S subunit for each of the three defined groups, early binders (green, S15), moderate binders (orange, S7), and late binders (red, S3). The early binders start with a relatively high protein level and start to increase in protein level in earlier fractions compared to moderate or late binders. Error bars represent the standard deviation of multiple measurements from different peptides or ions of the same protein. In the case where only one measurement was obtained, error bars are omitted. Fraction numbers correspond to Fig. 1b. (b) A Nomura assembly map color-coded based on the three groups. Early binders are represented with a green background, moderate binders are represented with an orange background, and late binders are represented with a red background. (c) Curves for representative proteins from the 50S subunit for each of the three defined groups, early binders (green, L4), moderate binders (orange, L5), and late binders (red, L35). (d) A Nierhaus assembly map color-coded based on the three groups. Early binders are represented with a green background, moderate binders are represented with an orange background, and late binders are represented with a red background.

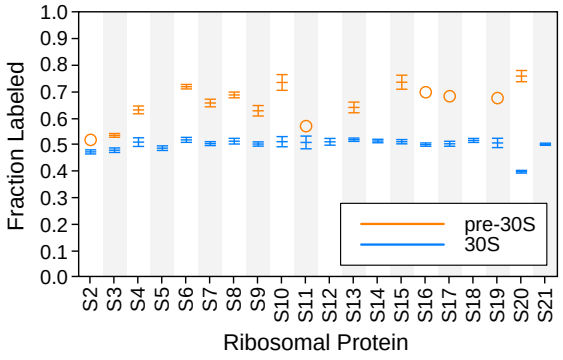

Fig. 4. Fraction labeled for the 21S intermediate and 30S subunit. Shown are values for a single sucrose gradient fraction from the 30S peak (blue; Fig. 1b, fraction 11) and the 21S peak (orange; Fig. 1b, fraction 6). Fraction labeled values for the 21S intermediate are generally higher than those for the 30S, but not 1.0 as expected. Error bars represent the standard deviation of multiple measurements from different peptides or ions of the same protein. In the case where only one measurement was obtained, a circle is used.

5–11, there is approximately a fourfold variation in the amount of 16S rRNA and only a twofold variation from fraction 6–11. From fraction 11–17, there is approximately a threefold variation in the amount of 23S rRNA. In both cases, the later fractions contain more rRNA and thus a higher number of intermediates or complete subunits, but each point in the continuum is significantly populated.

Incomplete particles contain proteins from previously existing intact subunits

The fraction of labeled protein was measured for both the 30S subunit and its 21S assembly intermediate using pulse-labeling (see Materials and Methods). Initially, a simultaneous pulse of neomycin and ^{15}N-labeled medium was used. While the 21S particles were significantly enriched with 50% ^{15}N-labeled proteins synthesized after this pulse, the levels were not as high as expected for a newly generated assembly intermediate that accumulates only after the pulse (data not shown). In order to ensure that the available pool of previously synthesized unlabeled ribosomal proteins was completely depleted before the onset of 21S accumulation, the initial medium was subsequently pulsed with ^{15}N-labeled media 10 min before the addition of neomycin. Since ribosomes assemble quickly *in vivo*[31] and the pool of free ribosomal proteins is small,[32] by the time 21S assembly intermediates begin to accumulate, no unlabeled proteins should remain available to these newly assembling particles. The 10-min period provides ample time to flush out the entire reserve of previously synthesized unlabeled ribosomal proteins. For the 30S subunit, the fraction labeled values are similar for all proteins (~0.5, Fig. 4) and reflect the relative amount of each protein that was synthesized before and after the isotope pulse.

Since the 21S assembly intermediate accumulates in the cell only after neomycin is added, it is expected to be composed entirely of newly synthesized 50% ^{15}N-labeled proteins and have a fraction labeled value of 1. Interestingly, the fraction labeled values for proteins in the 21S particle (~0.6–0.7) are higher than those for proteins in the 30S subunit (~0.5) but are significantly less than 1 (Fig. 4); hence, the 21S particles include unlabeled proteins that were synthesized before the isotope pulse and these unlabeled proteins must therefore have originated in previously intact 30S subunits.

Discussion

In previous analyses of ribosomes and ribosome assembly, the protein composition of ribosomal particles has been characterized using 2D gel electrophoresis and autoradiography, where the presence or absence of proteins can be confirmed. However, with such techniques, it is difficult to determine if the proteins are present in stoichiometric amounts. More recently, LC/MS has been used to quantify the protein levels in ribosomal particles by comparison of peak intensities.[22,33] In the current work, LC/MS-based quantitation is improved and extended to measure protein levels with high accuracy and sensitivity, detecting occupancies of less than 5% with multiple independent measurements for peptides from a single protein. These techniques provide a new level of rigorous quantitation and offer a new perspective on the composition and formation of these assembly intermediates.

The 30S assembly intermediate resulting from treatment with neomycin has been previously characterized,[25] but only by qualitative indication of the presence or absence of each protein. In this work, precise levels of all proteins were detected, making a direct comparison to the previous work difficult. This does serve to highlight the power of decoupling the identification procedure from the quantitation since such low levels of proteins can be measured.

Heterogeneous precursor particles and implications for assembly

Though the exact composition of the precursor particles remains unclear, the current work demonstrates that these particles are heterogeneous within each sucrose gradient fraction as indicated by the low and varied protein levels measured. Any fraction may contain particles where the presence

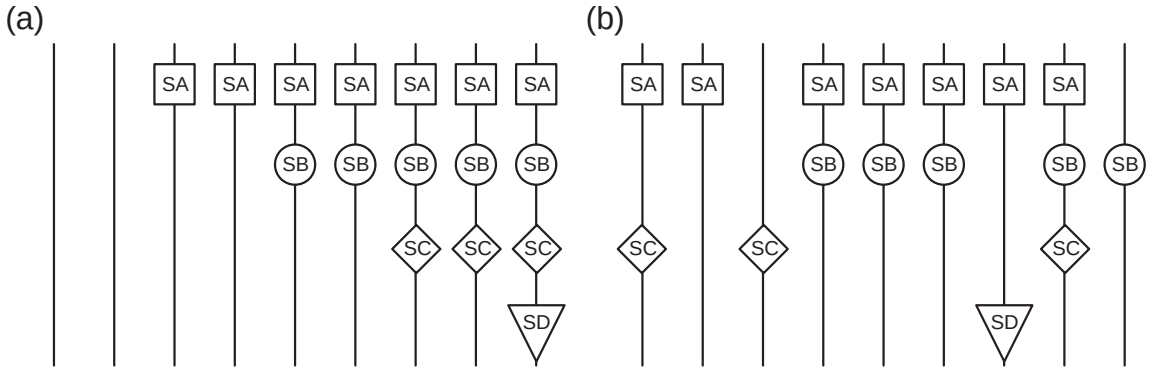

Fig. 5. Different ways to achieve the same bulk protein level. In these examples, consider the four hypothetical proteins SA (protein level 0.78), SB (0.56), SC (0.33), and SD (0.11). (a) Perfect correlation between proteins. SD depends on SC, which depends on SB, which depends on SA. The particles mimic a single assembly trajectory. (b) Imperfect correlation allows for the same bulk protein level but differences in composition at the molecular level. The particles mimic multiple parallel assembly trajectories.

of proteins is highly correlated, with one depending on another in an assembly-dependent manner as illustrated schematically in Fig. 5a, or the subsets of proteins may not be correlated, resulting in a statistical distribution of proteins across the rRNA molecules and a diverse set of particles, as illustrated in Fig. 5b. Recent data indicating that the 30S subunit assembles via multiple parallel assembly trajectories[12] suggest that the latter possibility is more likely. A single assembly pathway would result in a hierarchical progression of highly correlated particles while multiple parallel assembly pathways would generate a wide variety of particles each with a distinct complement of proteins as the particles build up in different ways.

Stability of assembly intermediates and comparison to RI

Intermediates of large macromolecular complexes are inherently less stable than the final product and some of the heterogeneity here may be the result of a statistical dissociation of loosely bound proteins from the partially assembled subunits, particularly during the sucrose gradient purification. However, the significant differences observed between previously characterized intermediates induced by different perturbations[18,19,22,34] indicate that the proteins and protein levels observed are inherent to the perturbation, in this case neomycin treatment. Though some small fraction of proteins may fall off during purification, the results are not simply a reflection of thermodynamic binding stabilities during ultracentrifugation. A comparison between the 21S assembly intermediate and RI[13] provides further support that the protein levels measured are not artifacts of the purification procedure. The protein levels of the two particles show significant differences, particularly in the 5′ domain (Fig. 6). The neomycin 21S and RI 21S particles were purified under almost identical conditions in the same laboratory, but exhibited distinctly different protein level profiles.

How proteins from previously synthesized 30S subunits are incorporated into the 21S assembly intermediate

Pulse-labeling experiments indicate that the pre-30S particles are, on average, newer than their intact counterparts, as they are composed of a higher proportion of labeled, post-isotope pulse proteins. These pre-30S particles accumulate only after the isotope pulse and are expected to be composed entirely of 50% ^{15}N-labeled proteins (Fig. 7a). Interestingly, they contain unlabeled proteins that must originate from ribosomal subunits synthesized before the addition of neomycin (Fig. 7b). There are several mechanisms by which these previously synthesized proteins may be incorporated into newly synthesized precursor particles. One possibility is that proteins may exchange between the intact subunits and the assembly intermediates (Fig. 7c). An exchange of unlabeled proteins from intact subunits to assembly intermediates would result in fraction labeled values <1.0 as observed. However, such an exchange would also be expected to result in covariation between fraction labeled values of the incomplete particles and the complete subunits and no such covariation (as evidenced by no concurrent increase in the fraction labeled value of complete subunits) is evident. This correlation might be obscured by the relatively low abundance of proteins in the 21S particle. A second possibility is that intact subunits may be degraded into particles of approximately the same size as the assembly intermediates (Fig. 7d). These would co-sediment with the assembly intermediates and would be

impossible to distinguish strictly based on the protein content. Analysis of ribosome degradation under starvation conditions has revealed several particles with a partial protein complement and degraded rRNA.[35,36] Combined with the understanding that the final steps in rRNA processing are believed to occur only after 30S and 50S subunits assemble into complete ribosomes, detailed analysis of the rRNA of these fractions may yield clues as to whether or not any of the particles are the result of degradation, though smaller rRNA species were not observed here (data not shown). Finally, under the conditions of neomycin stress, intact subunits may also be completely dismantled into individual proteins (Fig. 7e). If reused, these proteins would provide an available pool of unlabeled proteins for newly assembling subunits destined to accumulate in the cell as assembly intermediates. If this were the case, it suggests an interesting mechanism whereby the cell may be able to detect stalled ribosomes and reuse their components.

The molecular mechanism of neomycin, the disruption of ribosome assembly, and competency of precursor particles

One outstanding question is how neomycin affects ribosome assembly on a molecular level. Neomycin inhibits protein synthesis by binding to the A-site of the 16S rRNA,[37] and a secondary role has been proposed where neomycin inhibits assembly via a novel mechanism.[24] The results here show that ribosome assembly is generally disrupted in the presence of sublethal concentrations of neomycin

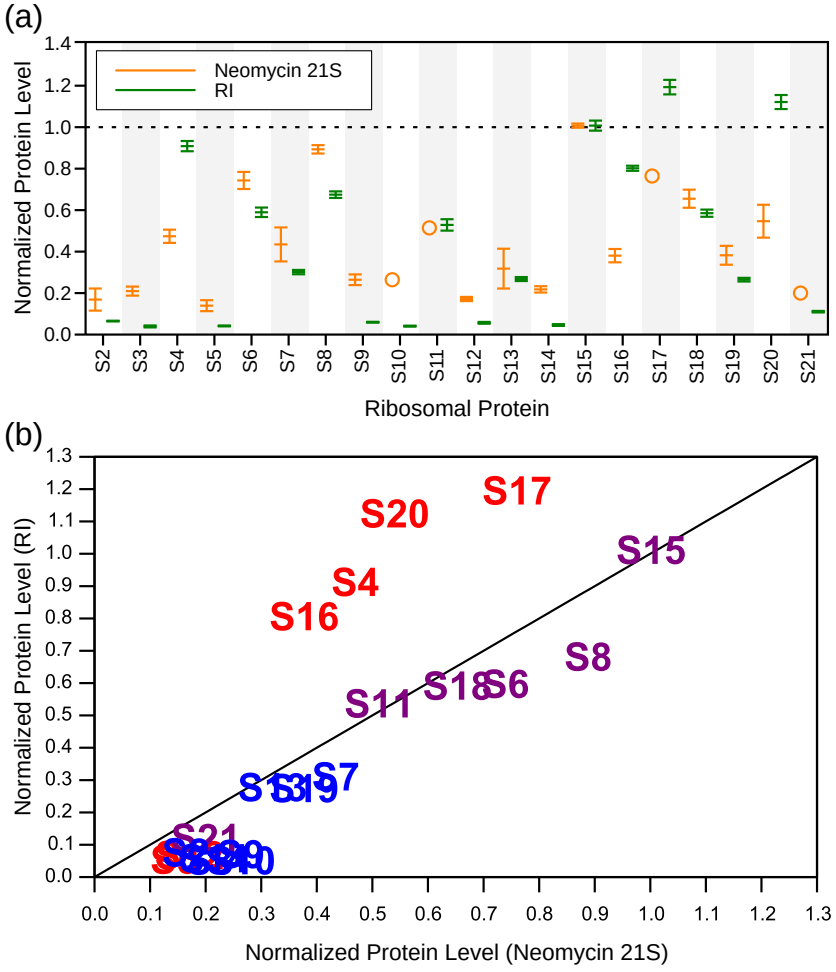

Fig. 6. Comparison of the neomycin-induced 21S assembly intermediate and RI. (a) Protein levels are normalized such that the value for S15 is 1.0 in both cases. Values for the neomycin 21S particle are in orange and values for RI are in green. The largest differences occur in the primary and secondary proteins of the 5′ domain (S4, S16, S17, and S20), which are present at relatively high levels in RI. (b) The same values plotted one against another. Data points are labeled by protein name and colored by domain (5′ domain in red, central domain in purple, 3′ domain in blue). Again, proteins S4, S6, S17, and S20 are clearly visible as different between the two particles.

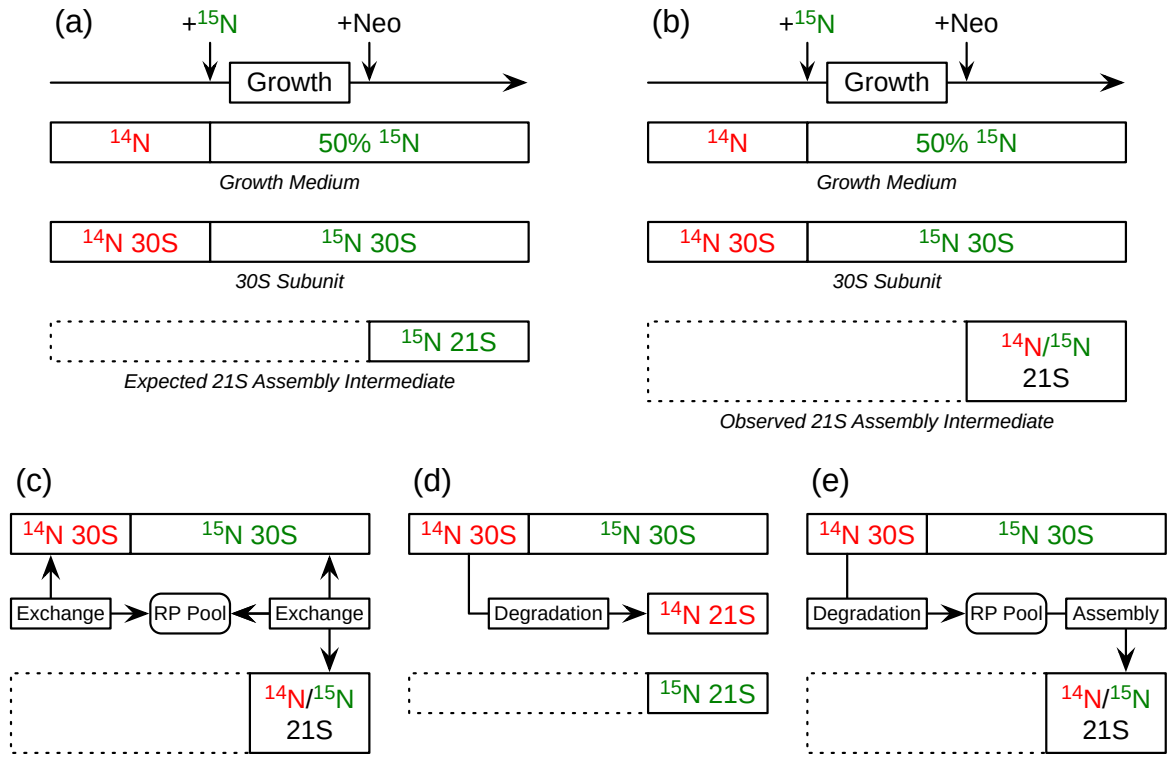

Fig. 7. Possible origins of the unlabeled proteins from previously assembled 30S subunits appearing in the 21S assembly intermediate. (a) Schematic of the isotope pulse experiment highlighting when the medium is unlabeled and 50% ^{15}N-labeled, and when the 21S intermediate begins to accumulate. Since the 21S particle only accumulates when the medium is ^{15}N-labeled, it is expected to be composed entirely of ^{15}N-labeled proteins. (b) An altered schematic showing the observed result. Rather than finding 21S particles containing only 50% ^{15}N-labeled proteins, 21S particles contain a mixture of unlabeled and 50% ^{15}N-labeled proteins. There are several possible explanations for the presence of unlabeled proteins in the 21S particle. (c) Proteins could exchange between 30S subunits and 21S particles via the free pool of ribosomal proteins (RP Pool). (d) Previously existing unlabeled 30S subunits could degrade into 21S particles of the same size as the assembly intermediates observed. (e) Unlabeled 30S subunits could be completely dismantled into their component proteins, and these unlabeled proteins made available to assembling 21S intermediates.

and that assembly of both 30S and 50S subunits is affected. Given the recent work showing that the effects of erythromycin and chloramphenicol on ribosome assembly are secondary effects of the inhibition of protein synthesis,[38] it is likely that the effects of neomycin on ribosome assembly are general secondary effects as well.

Previous work on both 30S and 50S assembly has demonstrated the existence of initiator proteins, whose presence is required for the formation of active subunits.[39,40] As all proteins are detected in both the 30S and 50S assembly intermediates, it does not appear as if neomycin excludes the binding of these initiator proteins, but it may interfere with subsequent RNA folding and protein binding during later stages of assembly. Nevertheless, the patterns of protein occupancy represent a true distribution of intermediates under these conditions that provides clues to the assembly process. The high protein level of central domain proteins compared to the 5′ domain primary binding proteins S4 and S20 is in contrast to *in vitro* kinetic studies of 30S subunit assembly[11] and the protein levels obtained for RI (Fig. 6). S4 and S20 are among the quickest binding proteins *in vitro* and are present at the highest levels in RI but are not present at the highest levels in the 21S assembly intermediate characterized here. This suggests that rather than simply slowing or stopping assembly at intermediate stages, the effects of neomycin may also bias the 30S assembly landscape towards nonnative trajectories; however, it remains unclear if the *in vitro* measurements truly reflect the kinetics of assembly in the cell. Some of this bias may also be a reflection of how the different ribosomal proteins are affected by the inhibition of protein synthesis. Synthesis of ribosomal proteins is highly regulated[41] and subject to complex regulatory cascades;[42] hence, it is feasible that one protein could be affected differently than another.

The precursor particles here may be on-pathway intermediates competent to become complete subunits, dead-end particles, or some combination of

the two. Diluting out the neomycin allows the cells to recover and rapid exponential growth to continue (data not shown). The fraction of labeled 30S subunits measured after neomycin is diluted should reflect the fraction of any labeled 21S particles that go on to be completed subunits and might show variations between the individual proteins such as those seen in the 21S particle (Fig. 4). Quantitative measurements after neomycin dilution do not show any protein-to-protein variability (data not shown), suggesting either that 21S neomycin particles do not go on to be complete 30S subunits or simply that the quantity of 21S particles that proceed to completion is too small to be detected. Indeed, the sucrose gradient of neomycin-treated *E. coli* (Fig. 1b) and gel electrophoresis results show fewer 21S particles than 30S subunits.

Concluding Remarks

The current work provides a framework for the detailed analysis of ribosomal particles that accumulate in the cell under conditions of perturbed growth and ribosome biogenesis. These particles are analyzed in terms of their protein composition and the temporal origin of their component proteins. A continuum of assembly intermediates for both the 30S and 50S subunits was discovered in the cell when treated with neomycin. These precursor particles were heterogeneous in composition, and the levels of different proteins increased at different rates across the continuum, allowing proteins to be classified into three distinct groups. Interestingly, the pre-30S particle contained a high level of central domain proteins that was not predicted by previous results. A fraction of the proteins present in these precursor particles originated in previously intact subunits, suggesting ribosome degradation or the reuse of ribosomal proteins.

The principles of the method are generally applicable to any system where ribosomal assembly intermediates can be isolated, including strains with assembly factor mutations or deletions. Studying a wide range of such intermediates will give insight into the various assembly trajectories of the ribosome *in vivo* and the wide variety of pathways and intermediates through which assembling ribosomes pass. While both the size and abundance of the ribosome facilitate purification of particles from cells, the

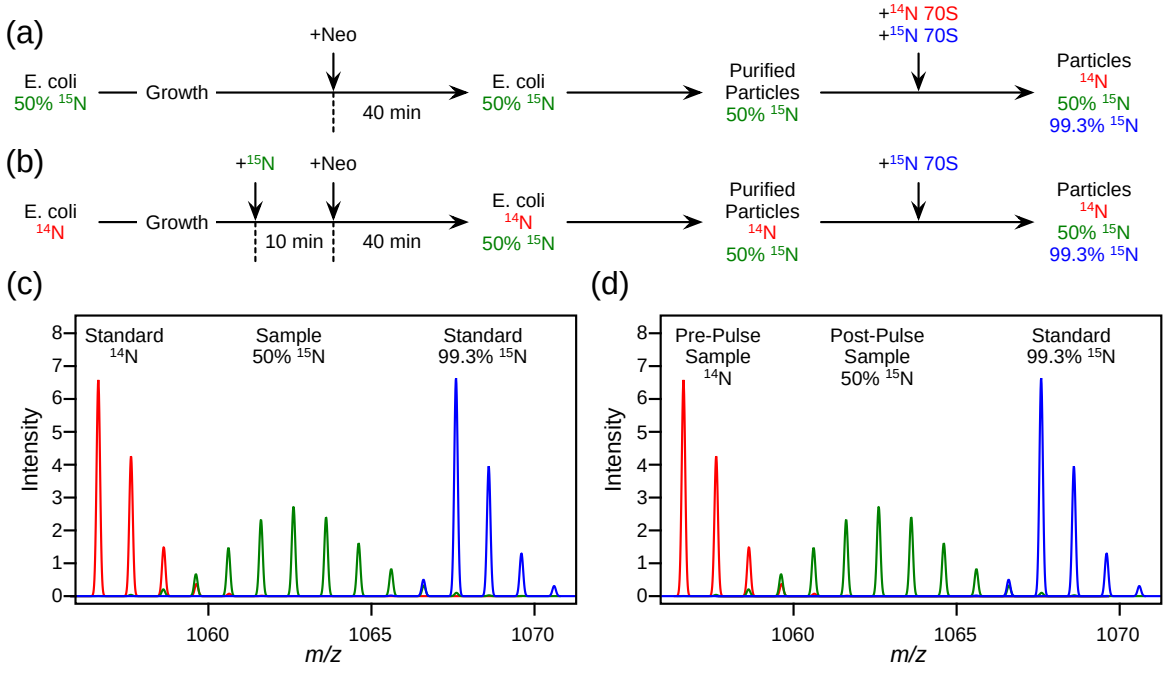

Fig. 8. Experimental design. (a) Schematic of a double-spike protein inventory experiment for quantifying protein levels. Neomycin is added to rapidly growing *E. coli* in 50% ^{15}N-labeled media; particles are purified on a sucrose gradient and combined with both unlabeled and fully ^{15}N-labeled ribosomes. (b) Schematic of an isotope pulse-labeling experiment to time-stamp ribosomal proteins. After pulsing with ^{15}N-labeled media, neomycin is added to rapidly growing *E. coli* and particles are purified on a sucrose gradient and combined with fully ^{15}N-labeled ribosomes as an external standard. (c) The resulting isotope distribution for the double-spike experiment consists of three parts, unlabeled (the first standard, red), 50% ^{15}N-labeled (the sample, green), and fully ^{15}N-labeled (the second standard, blue). (d) The resulting isotope distribution for the isotope pulse experiment consists of three parts, unlabeled (sample before the isotope pulse, red), 50% ^{15}N-labeled (sample after the isotope pulse, green), and fully ^{15}N-labeled (standard, blue).

techniques described here may be generally extended to the analysis of the assembly and turnover dynamics of other large complexes such as RNA polymerase, large proteasomes, or the spliceosome.

Materials and Methods

Experimental design of protein inventory and pulse-labeling methods

Two experiments are performed to characterize ribosome assembly intermediates that accumulate in bacteria. The first experiment is a protein inventory experiment, where the proteins present in a particle and their relative amounts are quantitated. One shortcoming for protein quantitation using mass spectrometry is the definitive treatment of proteins that are truly absent in the sample, since proteins can be missed for many experimental reasons in proteomics experiments.[43] This shortcoming can be circumvented if the identification procedure is carried out independently from the quantitation procedure using the same data set. This strategy is implemented here by using 50% ^{15}N-labeled particles for quantitation but a combination of unlabeled and fully ^{15}N-labeled ribosomes for identification.

In the protein inventory experiment (Fig. 8a), cells are grown to mid-log phase in 50% ^{15}N-labeled medium before they are pulsed with a sublethal concentration of neomycin. After an additional 40 min of growth, ribosomal subunits and assembly intermediates are separated by sucrose gradient ultracentrifugation. For each fraction from the gradient, unlabeled ribosomes and fully ^{15}N-labeled ribosomes are added as external standards. After trichloroacetic acid (TCA) precipitation to collect the proteins, the mixture is digested with trypsin and the resulting peptides are analyzed by LC/MS.

The protein inventory experiment provides quantitative information only about the amount of proteins present in a particle. Pulse-labeling is used to time-stamp proteins based on their time of synthesis in order to reveal the origins of the proteins incorporated into different particles. In the pulse-labeling experiment (Fig. 8b), cells are grown in unlabeled medium to mid-log phase before pulse-labeling by the addition of ^{15}N-labeled medium to a final concentration of 50% ^{15}N. During the ensuing 10-min period, all of the unlabeled ribosomal precursors are completely turned over and all of the newly synthesized ribosomes are 50% ^{15}N-labeled. After this 10-min clearance period, the cells are pulsed with neomycin to induce the formation of assembly intermediates. After an additional 40 min of growth, ribosomal subunits and assembly intermediates are purified via sucrose gradient ultracentrifugation. In this case, a single fully ^{15}N-labeled ribosomal standard is added to each fraction prior to TCA precipitation, trypsin digestion, and LC/MS analysis.

In both experiments, the resultant mass spectrum for a single peptide is composed of three isotope distributions: one unlabeled, one 50% ^{15}N-labeled, and one fully ^{15}N-labeled. In the protein inventory experiment, these are attributed to the unlabeled standard, the sample, and the labeled standard, respectively (Fig. 8c), while in the pulse-labeling experiment, these are attributed to proteins synthesized before the isotope pulse, proteins synthesized after the isotope pulse, and the single labeled external standard, respectively (Fig. 8d).

Cell growth for the protein inventory experiment

E. coli MRE600 cells (American Type Culture Collection strain 29417), lacking ribonuclease I, were grown at 37 °C in M9 glucose minimal medium supplemented with trace metals and vitamins. The medium was prepared with 0.5 g/L ^{14}N ammonium sulfate and 0.5 g/L ^{15}N ammonium sulfate as the sole nitrogen source. Cells were grown to OD_{600} (optical density at 600 nm) = 0.5–0.6 before a neomycin pulse of 15 μg/mL was added. The amount of neomycin was determined by pulsing varying amounts of neomycin into rapidly growing cultures (Supplementary Fig. S5). Under the conditions used here, 15 μg/mL of neomycin slowed but did not arrest growth. The cultures were then grown for an additional 40 min prior to harvest and ribosome preparation. Cells were harvested by centrifugation at 6000 rpm for 10 min and stored at −80 °C.

Cell growth for the isotope pulse experiment

E. coli MRE600 cells (American Type Culture Collection strain 29417), lacking ribonuclease I, were grown at 37 °C in M9 glucose minimal medium supplemented with trace metals and vitamins. The medium was prepared with 1 g/L ^{14}N ammonium sulfate as the sole nitrogen source. Cells were grown to OD_{600} = 0.4–0.5, pulsed by the addition of an equal volume of pre-warmed M9 minimal medium containing 1 g/L ^{15}N ammonium sulfate, and then grown for 10 min before a neomycin pulse of 15 μg/mL was added. The cultures were then grown for an additional 40 min prior to harvest and ribosome preparation. Cells were harvested by centrifugation at 6000 rpm for 10 min and stored at −80 °C.

Cell lysis and preparation

Frozen cell pellets were thawed and resuspended in low magnesium lysis buffer ["low magnesium, buffer A": 20 mM Tris–HCl, pH 7.5, 100 mM NH_4Cl, 1 mM $MgCl_2$, 0.5 mM ethylenediaminetetraacetic acid (EDTA), and 6 mM β-mercaptoethanol] and then lysed in a bead beater (BioSpec Products, Inc., Bartlesville, OK) using 0.1-mm zirconia/silica beads. Insoluble debris was removed by two centrifugation steps: a low-speed spin at 6000 rpm for 10 min and then a high-speed spin centrifugation step at 16,000 rpm (31,000*g*) for 40 min. A 1-mL aliquot of the supernatant was layered onto a 35-mL 10–40% sucrose gradient (50 mM Tris–HCl, pH 7.8, 1 mM $MgCl_2$, and 100 mM NH_4Cl) in a SW 32 rotor (Beckman Coulter, Fullerton, CA) by spinning at 26,000 rpm at 4 °C for 16 h in order to separate out subunits and intermediates. The gradients were fractionated with a Brandel fractionator. Subunit concentration in the fractions was estimated by measuring the optical density at 260 nm.

The protein inventory experiments were performed four times using two different spike conditions, and the data shown are a representative replicate. The first

conditions used 150 pmol of sample for pre-30S fractions, adding 15 pmol of both ^{14}N 70S* and ^{15}N 70S* to each fraction. For all other fractions, 50 pmol of sample was used and 25 pmol of ^{14}N 70S* and ^{15}N 70S* was added to all other fractions.

The second set of conditions used 150 pmol of sample for pre-30S fractions, adding 30 pmol of both ^{14}N 70S* and ^{15}N 70S* to each fraction. For all other fractions, 100 pmol of sample was used and 20 pmol of ^{14}N 70S* and ^{15}N 70S* was added to all other fractions.

The pulse experiments were performed two times using 150 pmol of sample for pre-30S fractions and added 15 pmol of ^{15}N 70S* to pre-30S fractions, and the data shown are a representative replicate. For all other fractions, 50 pmol of sample was used and 25 pmol of ^{15}N 70S* was added to all other fractions. The proteins were then precipitated by adding 6.1 M TCA to a final concentration of 13%.

Samples were incubated on ice for 4–6 h. The protein precipitate was pelleted by centrifugation at 13,000*g* for 20 min at 4 °C. The supernatant was removed and the pellets were rinsed first with 10% TCA and then with ice-cold acetone, dried in a Speed-Vac concentrator, and then resuspended in 20 μL of 100 mM ammonium bicarbonate (pH 8.5) in 5% acetonitrile (ACN). A 2-μL aliquot of 50 mM DTT was added, and the samples were incubated at 65 °C for 10 min. Cysteine residues were modified by the addition of 2 μL of 100 mM iodoacetamide followed by incubation at 30 °C for 30 min in the dark. Proteolytic digestion of the 30S proteins was carried out by the addition of 2 μL of 0.1 μg/mL modified sequencing grade porcine trypsin (Promega, Co., Madison, WI) with incubation overnight at 37 °C. Undigested proteins were precipitated by adding 1/3 volume of 20% ACN in 2% trifluoroacetic acid and removed by centrifugation. The supernatant was loaded to a PepClean C18 spin column (Thermo Fisher Scientific Inc., Rockford, IL) to remove salts and concentrate the samples. The eluant was dried in a Speed-Vac concentrator and the peptides were redissolved in 10 μL of 5% ACN in 0.1% formic acid. An 8 μL of aliquot was used for the electrospray ionization time of flight (ESI-TOF) analysis.

Unlabeled ^{14}N 70S* and labeled ^{15}N 70S* ribosomes were prepared by growing *E. coli* MRE600 cells in either ^{14}N or ^{15}N M9 minimal media, respectively. Cells were lysed in high magnesium lysis buffer (20 mM Tris–HCl, pH 7.5, 100 mM NH_4Cl, 10 mM $MgCl_2$, 0.5 mM EDTA, and 6 mM β-mercaptoethanol) according to the above protocol and insoluble debris was removed as described above. The supernatant was layered onto a 5-mL cushion of 37.7% sucrose in buffer B (20 mM Tris–HCl, pH 7.5, 500 mM NH_4Cl, 10 mM $MgCl_2$, and 0.5 mM EDTA) and the 70S ribosomes were pelleted by spinning at 37,200 rpm at 4 °C in a Ti70.1 rotor (Beckman Coulter) for 22 h. The supernatant was removed, the tube and the 70S ribosome pellet was rinsed with 70S buffer (50 mM Tris–HCl, pH 7.8, 10 mM $MgCl_2$, 100 mM NH_4Cl, and 6 mM β-mercaptoethanol), and the pellet was resuspended in 70S buffer. Aliquots were frozen and stored at −20 °C.

Agarose gel electrophoresis

Sucrose gradient fractions were run on a 1% agarose gel to verify the presence and size of rRNA. A 1% agarose gel with ethidium bromide was poured in a large 40-lane gel box (13 cm × 16.5 cm) in 1× Tris–acetate, EDTA. Samples were set up with 6 μl of sucrose fraction (RNA), 4 μl of water, and 2 μl of 6× agarose dye. A 1 DNA ladder was used as a reference. A total of 10 μL of sample mixture was loaded onto the gel for each fraction and run at 150 V for 1.5 h in 1× Tris–acetate, EDTA running buffer. The gels were viewed at 312 nm on a Gibco BRL UV transilluminator to identify RNA bands.

ESI-TOF mass spectrometry

The peptide samples were analyzed on an Agilent 1100 Series HPLC instrument coupled to an Agilent ESI-TOF instrument with capillary flow electrospray (Agilent Technologies Inc., Santa Clara, CA). The digested ribosomal proteins were injected using an autosampler onto an Agilent Zorbax SB C18 150 mm × 0.5 mm HPLC column. The mobile phases used were buffer A (H_2O, 0.1% formic acid) and buffer B (ACN, 0.1% formic acid). Peptides were separated on an ACN gradient in 0.1% formic acid at a flow rate of 7 μL/min. The steps of the gradient were 5–15% ACN over 10 min, 15–50% ACN over 70 min, and 50–95% ACN over 4 min. Data were collected over the m/z range of 300–1300.

MS data processing and feature identification

A flowchart providing a brief overview of the analysis procedure is given in Supplementary Fig. S6. A feature list was generated using the Agilent programs Mass Hunter and Mass Profiler. To generate the feature list, Mass Hunter (version 1.0.0.0, A.02.00) was used to read an Agilent .wiff file and generate a .mhd file (signal-to-noise threshold of 3 and "Peptidic isotope distribution" enabled, default parameters otherwise). Mass Profiler (version 1.0.2068.18614) was used to read the .mhd file and export a feature list using the "Export acquired included list" function (default software parameters). Subsequent processing steps were performed using in-house software. A feature corresponds to the entire isotopic envelope from a single ion and contains both a monoisotopic peak and several isotopomers. Features are defined by the m/z value of the monoisotopic peak, the charge of the ion, and the retention time on the column.

Peptides are first identified using a procedure previously developed for quantifying isotope pulse-chase experiments *in vitro*[11,44,45] and subsequently extended to experiments *in vivo*.[42] The feature list was compared to a theoretical trypsin digest of all ribosomal proteins from the *E. coli* 70S ribosome (S2–S21 and L1–L36). The theoretical trypsin digest includes peptides with up to two consecutive missed cleavages and includes both unlabeled and fully ^{15}N-labeled forms of the resultant peptides, at charge states up to +6. Cysteine residues were all treated as modified by iodoacetamide. Experimental features were assigned possible identities based on matches in the theoretical digest of the charge state and mass within a 20 ppm tolerance. An instrument-based accuracy offset was determined using the entire data set, with each MS data set adjusted individually. Feature pairs corresponding to ^{14}N and ^{15}N versions of the same peptide were extracted from the feature list when the two features exhibited the same retention time within 0.1 min. When

multiple peptide identities matched the same features, or when the same peptide matched multiple proteins, the features were removed from further consideration.

Using this approach for the protein inventory experiment, multiple peptides can be unambiguously identified for each protein based solely on the peaks from the two intact ribosome external standards. Feature pairs from the unlabeled and fully labeled standards are present in the mass spectrum for each protein. Thus, even if a protein is completely absent in the sample, the standards will still generate feature pairs and allow for unequivocal confirmation of the protein's absence by an amplitude of zero for the 50% ^{15}N-labeled distribution. An example showing the standards-based identification of a peptide when the protein is absent from the sample is shown in Supplementary Fig. S7.

To enable quantitative analysis of the data for each of the feature pairs, we converted the full raw data set in the Agilent ".wiff" format to a text file using the program Analyst QS (Applied Biosystems/MDS Sciex, build 7222) and the "Data File Export" function (store profile data above 0 counts, default parameters otherwise). For each identified feature pair, the data range including the entire isotopic envelope for both features in the m/z dimension and 0.2 min centered about the average retention time in the time dimension were extracted from the full data set.

Determination of amplitudes of peptide species

Theoretical isotope distributions were fit to these extracted spectra using the program isodist.[30] Isodist uses least-squares Fourier transform convolution to fit calculated isotope distributions to the entire isotopic envelope observed in the mass spectrum. Three distributions were fit, one unlabeled (all isotope values given by natural abundance), one partially labeled (^{15}N fixed at 50%), and one fully labeled (^{15}N fixed at 99.3%) to the experimental spectra. An example of such a fit is shown in Supplementary Fig. S8. The amplitudes given by isodist yield the relative amounts of unlabeled, 50% ^{15}N-labeled, and ^{15}N-labeled peptide in the sample and can be used to calculate either protein level or fraction of labeled protein (see below).

For the protein inventory experiment, since both the unlabeled and fully labeled amplitudes depend on the amount of standard added and the standards contain stoichiometric amounts of all proteins, there is expected to be a linear relationship between the two amplitudes for all peptides. A plot of the relationship between these two amplitudes for a single experiment is shown in Supplementary Fig. S9. This method has previously been validated for its accuracy and applicability to macromolecular assembly kinetics.[11,30,42,44,45]

The fits for all extracted spectra were evaluated visually for goodness of fit, and those with poorly fitting theoretical distributions were eliminated. Poor fits typically arise from either noise in the mass spectrum or overlap of the isotope distributions from co-eluting peptides with a similar mass/charge ratio. Spurious feature pairs generated from misidentification of a ^{14}N feature as a ^{15}N feature are easily eliminated at this step due to the distinctive isotopic envelope of a ^{15}N-labeled peptide. For most proteins, multiple peptides are identified, and the standard deviations of the fraction labeled values for the set of peptides provide an estimate of the error for quantitation of each protein.

Definition of protein level and fraction labeled

Two separate quantities can be defined. In the protein inventory experiment, the relative protein level is defined as

$$P = \frac{A_L}{A_U + A_F}$$

where A_U, A_L, and A_F refer to the unlabeled, 50% ^{15}N-labeled, and fully ^{15}N-labeled amplitudes, respectively. The relative protein level is the amount of protein in the sample compared to the sum of the two standards. In the second experiment, the fraction labeled is defined as

$$f = \frac{A_L}{A_U + A_L}$$

The fraction labeled defines the amount of protein that was synthesized after the isotope pulse as a fraction of the total amount of protein present in the sample.

Scaling of protein levels

The initial protein levels calculated depend implicitly on the amount of external standard added, and these values must be scaled to yield the protein occupancy relative to the amount of rRNA. The scaled protein level P_{scale} is obtained by dividing the raw protein level P by a scaling factor R.

$$P_{scale} = \frac{P}{R}$$

The value for R can be derived from a reference fraction that is arbitrarily scaled such that the average protein level is 1.0. For the 30S subunit and the pre-30S intermediate, a single fraction from the center of the 30S peak was chosen, which is expected to contain complete, homogenous 30S subunits (Fig. 1b, fraction 10). Likewise, for the 50S subunit and the pre-50S intermediate, a single fraction from the center of the 50S peak was chosen (Fig. 1b, fraction 16). The scaling factor for this reference fraction (R_{ref}) relates to the scaling factor for a given fraction (R_i) by the following equation:

$$R_i = R_{ref}\frac{N_i}{N_{ref}}$$

where N_i is the total amount of rRNA used for LC/MS analysis in fraction i and N_{ref} is the total amount used for the reference fraction, assuming the amount of external 70S standard is the same. If twice as much material is used in fraction 1 compared to fraction 2, R_1 will be double R_2. Given the same raw protein level ($P_1 = P_2$), the scaled protein levels will also differ by a factor of 2 ($P_{scale,1} = 0.5 \cdot P_{scale,2}$). The total amount of rRNA used can be calculated from the volume and concentration of a fraction. The volumes are determined experimentally and the concentrations are determined relative to the reference fraction by quantitation of rRNA bands from agarose gel electrophoresis.

Reconstitution of RI and RI protein levels

In vitro reconstitutions were carried out using native 16S rRNA and a mixture of small ribosomal proteins S2–S21 (TP30) was prepared as previously described.[46] The final reaction conditions were 0.3 μM 16S rRNA, 0.45 μM TP30, 25 mM Tris–HCl, pH 7.5, 330 mM KCl, 20 mM $MgCl_2$, and 2 mM DTT. Two *in vitro* reconstitutions were performed at 40 °C to produce 30S subunits and two *in vitro* reconstitutions were performed at 4 °C to produce RI. The reconstitutions were performed as previously described.[10,11] The low temperature reconstitution to produce RI was assembled from 16S rRNA and a single pulse of excess unlabeled TP30, while the standard temperature reaction was produced using 16S rRNA and a single pulse of fully ^{15}N-labeled TP30. Both reactions were incubated separately for 1 h at their designated temperature and then purified separately on a 10–30% sucrose gradient by ultracentrifugation at 35,000 rpm for 9 h at 4 °C in an SW 41 rotor (Beckman Coulter). The gradients were fractionated at 0.75 ml/min with a Brandel fractionator, monitored at A_{254}, and either the 30S or RI (21S) peak was collected. The fractions from the collected peaks were then pooled and ODs were taken to determine the total amount of rRNA present. Equal amounts of the low-temperature RI/21S (^{14}N) and the high-temperature 30S (^{15}N) sample were then combined together. TCA precipitation, trypsin digestion, and mass spectrometry were performed as described above. Theoretical isotope distributions and data analysis were also performed as described above, with the protein level for RI defined as

$$P = \frac{A_U}{A_F}$$

where A_U and A_F refer to unlabeled (RI) and fully ^{15}N-labeled (30S) amplitudes, respectively. In this form, the protein level (P) gives the protein occupancy of the RI particle relative to the 30S subunits obtained by *in vitro* reconstitution.

Acknowledgements

This work was supported by grants from the National Institutes of Health (F32-GM083510 to M.T.S., F32-GM087858 to Z.S., and R37-GM053757 to J.R.W.). The authors wish to thank Stephen Chen for helpful discussions regarding pulse-labeling.

Supplementary Data

Supplementary data to this article can be found online at doi:10.1016/j.jmb.2010.08.005

References

1. Schuwirth, B. S., Borovinskaya, M. A., Hau, C. W., Zhang, W., Vila-Sanjurjo, A., Holton, J. M. & Cate, J. H. D. (2005). Structures of the bacterial ribosome at 3.5 Å resolution. *Science*, **310**, 827–834.
2. Selmer, M., Dunham, C. M., Murphy, F. V., Weixlbaumer, A., Petry, S., Kelley, A. C. *et al.* (2006). Structure of the 70S ribosome complexed with mRNA and tRNA. *Science*, **313**, 1935–1942.
3. Korostelev, A., Trakhanov, S., Laurberg, M. & Noller, H. F. (2006). Crystal structure of a 70S ribosome–tRNA complex reveals functional interactions and rearrangements. *Cell*, **126**, 1065–1077.
4. Mizushima, S. & Nomura, M. (1970). Assembly mapping of 30S ribosomal proteins from *E. coli*. *Nature*, **226**, 1214–1218.
5. Nomura, M. (1973). Assembly of bacterial ribosomes. *Science*, **179**, 864–873.
6. Herold, M. & Nierhaus, K. H. (1987). Incorporation of six additional proteins to complete the assembly map of the 50 S subunit from *Escherichia coli* ribosomes. *J. Biol. Chem.* **262**, 8826–8833.
7. Wilson, D. N. & Nierhaus, K. H. (2007). The weird and wonderful world of bacterial ribosome regulation. *Crit. Rev. Biochem. Mol. Biol.* **42**, 187–219.
8. de Narvaez, C. C. & Schaup, H. W. (1979). In vivo transcriptionally coupled assembly of *Escherichia coli* ribosomal subunits. *J. Mol. Biol.* **134**, 1–22.
9. Lewicki, B. T., Margus, T., Remme, J. & Nierhaus, K. H. (1993). Coupling of rRNA transcription and ribosomal assembly in vivo. Formation of active ribosomal subunits in *Escherichia coli* requires transcription of rRNA genes by host RNA polymerase which cannot be replaced by bacteriophage T7 RNA polymerase. *J. Mol. Biol.* **231**, 581–593.
10. Talkington, M. W. T., Siuzdak, G. & Williamson, J. R. (2005). An assembly landscape for the 30S ribosomal subunit. *Nature*, **438**, 628–632.
11. Bunner, A. E., Trauger, S. A., Siuzdak, G. & Williamson, J. R. (2008). Quantitative ESI-TOF analysis of macromolecular assembly kinetics. *Anal. Chem.* **80**, 9379–9386.
12. Adilakshmi, T., Bellur, D. L. & Woodson, S. A. (2008). Concurrent nucleation of 16S folding and induced fit in 30S ribosome assembly. *Nature*, **455**, 1268–1272.
13. Traub, P. & Nomura, M. (1969). Structure and function of *Escherichia coli* ribosomes. VI. Mechanism of assembly of 30 s ribosomes studied in vitro. *J. Mol. Biol.* **40**, 391–413.
14. Held, W. A. & Nomura, M. (1973). Rate determining step in the reconstitution of *Escherichia coli* 30S ribosomal subunits. *Biochemistry*, **12**, 3273–3281.
15. Holmes, K. L. & Culver, G. M. (2005). Analysis of conformational changes in 16 S rRNA during the course of 30 S subunit assembly. *J. Mol. Biol.* **354**, 340–357.
16. Holmes, K. L. & Culver, G. M. (2004). Mapping structural differences between 30S ribosomal subunit assembly intermediates. *Nat. Struct. Mol. Biol.* **11**, 179–186.
17. Sykes, M. T. & Williamson, J. R. (2009). A complex assembly landscape for the 30S ribosomal subunit. *Annu. Rev. Biophys.* **38**, 197–215.
18. Charollais, J., Pflieger, D., Vinh, J., Dreyfus, M. & Iost, I. (2003). The DEAD-box RNA helicase SrmB is involved in the assembly of 50S ribosomal subunits in *Escherichia coli*. *Mol. Microbiol.* **48**, 1253–1265.

19. Charollais, J., Dreyfus, M. & Iost, I. (2004). CsdA, a cold-shock RNA helicase from *Escherichia coli*, is involved in the biogenesis of 50S ribosomal subunit. *Nucleic Acids Res.* **32**, 2751–2759.
20. Al Refaii, A. & Alix, J. H. (2009). Ribosome biogenesis is temperature-dependent and delayed in *Escherichia coli* lacking the chaperones DnaK or DnaJ. *Mol. Microbiol.* **71**, 748–762.
21. Jiang, M., Datta, K., Walker, A., Strahler, J., Bagamasbad, P., Andrews, P. C. & Maddock, J. R. (2006). The *Escherichia coli* GTPase CgtAE is involved in late steps of large ribosome assembly. *J. Bacteriol.* **188**, 6757–6770.
22. Sharpe Elles, L. M., Sykes, M. T., Williamson, J. R. & Uhlenbeck, O. C. (2009). A dominant negative mutant of the *E. coli* RNA helicase DbpA blocks assembly of the 50S ribosomal subunit. *Nucleic Acids Res.* **37**, 6503–6514.
23. Mehta, R. & Champney, W. S. (2002). 30S ribosomal subunit assembly is a target for inhibition by aminoglycosides in *Escherichia coli*. *Antimicrob. Agents Chemother.* **46**, 1546–1549.
24. Mehta, R. & Champney, W. S. (2003). Neomycin and paromomycin inhibit 30S ribosomal subunit assembly in *Staphylococcus aureus*. *Curr. Microbiol.* **47**, 237–243.
25. Foster, C. & Champney, W. S. (2008). Characterization of a 30S ribosomal subunit assembly intermediate found in *Escherichia coli* cells growing with neomycin or paromomycin. *Arch. Microbiol.* **189**, 441–449.
26. Champney, W. S. & Burdine, R. (1995). Macrolide antibiotics inhibit 50S ribosomal subunit assembly in *Bacillus subtilis* and *Staphylococcus aureus*. *Antimicrob. Agents Chemother.* **39**, 2141–2144.
27. Chittum, H. S. & Champney, W. S. (1995). Erythromycin inhibits the assembly of the large ribosomal subunit in growing *Escherichia coli* cells. *Curr. Microbiol.* **30**, 273–279.
28. Snijders, A. P. L., de Vos, M. G. J. & Wright, P. C. (2005). Novel approach for peptide quantitation and sequencing based on ^{15}N and ^{13}C metabolic labeling. *J. Proteome Res.* **4**, 578–585.
29. Nelson, C. J., Huttlin, E. L., Hegeman, A. D., Harms, A. C. & Sussman, M. R. (2007). Implications of ^{15}N-metabolic labeling for automated peptide identification in *Arabidopsis thaliana*. *Proteomics*, **7**, 1279–1292.
30. Sperling, E., Bunner, A. E., Sykes, M. T. & Williamson, J. R. (2008). Quantitative analysis of isotope distributions in proteomic mass spectrometry using least-squares Fourier transform convolution. *Anal. Chem.* **80**, 4906–4917.
31. Lindahl, L. (1975). Intermediates and time kinetics of the in vivo assembly of *Escherichia coli* ribosomes. *J. Mol. Biol.* **92**, 15–37.
32. Marvaldi, J., Pichon, J., Delaage, M. & Marchis-Mouren, G. (1974). Individual ribosomal protein pool size and turnover rate in *Escherichia coli*. *J. Mol. Biol.* **84**, 83–96.
33. Iost, I., Charollais, J., Vinh, J. & Pflieger, D. (2008). Characterization of *E. coli* ribosomal particles: combined analysis of whole proteins by mass spectrometry and of proteolytic digests by liquid chromatography–tandem mass spectrometry. *Methods Mol. Biol.* **432**, 321–341.
34. Kaberdina, A. C., Szaflarski, W., Nierhaus, K. H. & Moll, I. (2009). An unexpected type of ribosomes induced by kasugamycin: a look into ancestral times of protein synthesis? *Mol. Cell*, **33**, 227–236.
35. Kaplan, R. & Apirion, D. (1975). The fate of ribosomes in *Escherichia coli* cells starved for a carbon source. *J. Biol. Chem.* **250**, 1854–1863.
36. Maruyama, H. B. & Okamura, S. (1972). Ribosome degradation and the degradation products in starved *Escherichia coli*. V. Ribonucleoprotein particles from glucose-starved cells. *J. Bacteriol.* **110**, 442–446.
37. Borovinskaya, M. A., Pai, R. D., Zhang, W., Schuwirth, B. S., Holton, J. M., Hirokawa, G. *et al.* (2007). Structural basis for aminoglycoside inhibition of bacterial ribosome recycling. *Nat. Struct. Mol. Biol.* **14**, 727–732.
38. Siibak, T., Peil, L., Xiong, L., Mankin, A., Remme, J. & Tenson, T. (2009). Erythromycin- and chloramphenicol-induced ribosomal assembly defects are secondary effects of protein synthesis inhibition. *Antimicrob. Agents Chemother.* **53**, 563–571.
39. Nowotny, V. & Nierhaus, K. H. (1982). Initiator proteins for the assembly of the 50S subunit from *Escherichia coli* ribosomes. *Proc. Natl Acad. Sci. USA*, **79**, 7238–7242.
40. Nowotny, V. & Nierhaus, K. H. (1988). Assembly of the 30S subunit from *Escherichia coli* ribosomes occurs via two assembly domains which are initiated by S4 and S7. *Biochemistry*, **27**, 7051–7055.
41. Zengel, J. M. & Lindahl, L. (1994). Diverse mechanisms for regulating ribosomal protein synthesis in *Escherichia coli*. *Prog. Nucleic Acid Res. Mol. Biol.* **47**, 331–370.
42. Sykes, M. T., Sperling, E., Chen, S. S. & Williamson, J. R. (2010). Quantitation of the ribosomal protein autoregulatory network using mass spectrometry. *Anal. Chem.* **82**, 5038–5045.
43. Ong, S. E. & Mann, M. (2005). Mass spectrometry-based proteomics turns quantitative. *Nat. Chem. Biol.* **1**, 252–262.
44. Bunner, A. E., Beck, A. H. & Williamson, J. R. (2010). Kinetic cooperativity in *Escherichia coli* 30S ribosomal subunit reconstitution reveals additional complexity in the assembly landscape. *Proc. Natl Acad. Sci. USA*, **107**, 5417–5422.
45. Bunner, A. E., Nord, S., Wikström, P. M. & Williamson, J. R. (2010). The effect of ribosome assembly cofactors on in vitro 30S subunit reconstitution. *J. Mol. Biol.* **398**, 1–7.
46. Staehelin, T. & Maglott, D. (1971). Preparation of *Escherichia coli* ribosomal subunits active in polypeptide synthesis. *Methods Enzymol.* **20**, 449–456.